



Quantifying spatial heterogeneity of vulnerability to short-term PM_{2.5} exposure with data fusion framework[☆]

Cheng-Pin Kuo^a, Joshua S. Fu^{a,*}, Pei-Chih Wu^{b,d}, Tain-Junn Cheng^c, Tsu-Yun Chiu^d, Chun-Sheng Huang^e, Chang-Fu Wu^{e,f}, Li-Wei Lai^d, Hsin-Chih Lai^{b,d}, Ciao-Kai Liang^g

^a Department of Civil and Environmental Engineering, University of Tennessee Knoxville, Knoxville, TN, USA

^b Department of Green Energy and Environmental Resources, Chang Jung Christian University, Tainan, Taiwan

^c Departments of Neurology and Occupational Medicine, Chi-Mei Medical Center, Tainan, Taiwan

^d Environmental Research and Information Center, Chang Jung Christian University, Tainan, Taiwan

^e Institute of Environmental and Occupational Health Sciences, National Taiwan University, Taipei, Taiwan

^f Department of Public Health, National Taiwan University, Taipei, Taiwan

^g Department of Air Quality Protection and Noise Control, Environmental Protection Administration, Taiwan

ARTICLE INFO

Keywords:

Fine particles
Disease burden
Emergency department visits
Mixed land-use patterns

ABSTRACT

The current estimations of the burden of disease (BD) of PM_{2.5} exposure is still potentially biased by two factors: ignorance of heterogeneous vulnerabilities at diverse urbanization levels and reliance on the risk estimates from existing literature, usually from different locations. Our objectives are (1) to build up a data fusion framework to estimate the burden of PM_{2.5} exposure while evaluating local risks simultaneously and (2) to quantify their spatial heterogeneity, relationship to land-use characteristics, and derived uncertainties when calculating the disease burdens. The feature of this study is applying six local databases to extract PM_{2.5} exposure risk and the BD information, including the risks of death, cardiovascular disease (CVD), and respiratory disease (RD), and their spatial heterogeneities through our data fusion framework. We applied the developed framework to Tainan City in Taiwan as a use case estimated the risks by using 2006–2016 emergency department visit data, air quality monitoring data, and land-use characteristics and further estimated the BD caused by daily PM_{2.5} exposure in 2013. Our results found that the risks of CVD and RD in highly urbanized areas and death in rural areas could reach 1.20–1.57 times higher than average. Furthermore, we performed a sensitivity analysis to assess the uncertainty of BD estimations from utilizing different data sources, and the results showed that the uncertainty of the BD estimations could be contributed by different PM_{2.5} exposure data (20–32%) and risk values (0–86%), especially for highly urbanized areas. In conclusion, our approach for estimating BD based on local databases has the potential to be generalized to the developing and overpopulated countries and to support local air quality and health management plans.

1. Introduction

The associations between exposure to ambient fine particulate matter (PM_{2.5}, particles with aerodynamic diameters under 2.5 μm) and increased risks of adverse health effects such as premature death, cardiovascular disease (CVD), and respiratory disease (RD) has been intensively investigated for decades (Apte et al., 2018; Wang et al., 2015a,b; Xing et al., 2016). The burden of disease (BD) is a commonly used assessment tool to quantify the impact of ambient PM_{2.5} exposure to human health and provide references for air quality and health

management. For example, the Global Burden of Disease (GBD) estimated that about 2.94 million deaths in 2017 could be attributed to particulate matter pollution (GBD, 2017 Risk Factor GBD 2017 Risk Factor Collaborators, 2018).

Technically, the BD can be estimated by either concentration-response functions (CRFs) (Ding et al., 2015; Qiu et al., 2015; Wang et al., 2015a,b) or integrated exposure-response functions (IERs) (Apte et al., 2015; Burnett et al., 2014), both of which use similar algorithms and have been applied intensively in previous studies. While the applied risks in CRFs tend to be constant (Ding et al., 2016), IERs parameterize

[☆] This paper has been recommended for acceptance by Admir C. Targino.

* Corresponding author. Department of Civil and Environmental Engineering, the University of Tennessee, 851 Neyland Drive, Knoxville, TN, 37996, USA.

E-mail address: jsfu@utk.edu (J.S. Fu).

the dependence of risks on $PM_{2.5}$ concentration from a meta-analysis of epidemiological studies (Burnett et al., 2014). In general, although these algorithms can provide reasonable BD estimations based on literature-based relative risks (RRs) and modeled/monitored $PM_{2.5}$ concentrations, the BD estimations still remain biased due to the algorithm assumptions.

One potential concern is that most studies employed risk values from other literature or reports to estimate the burden without assessing the representativeness of the study subjects or sampling bias of the reference, which could limit the application of the risk values or cause bias if the risk values were inappropriately applied. Another concern is that the spatial heterogeneity of risks among urban and rural areas were overlooked during the BD calculation. Most BD estimations at the country or regional level neglected the potential uncertainties derived from different vulnerabilities associated with living in diverse urbanization levels, for which differences in risk were related to neighboring land-use patterns and individual activity patterns (Barton, 2009; Ebisu et al., 2011; Son et al., 2015; Wernham, 2011) and have been identified in previous studies (Garcia et al., 2016; McGuinn et al., 2017). Among areas with diverse urbanization levels, $PM_{2.5}$ mass concentration and compositions adjacent to emission sources such as main roads and industrial complexes have higher $PM_{2.5}$ toxicity contributed by diesel particles, heavy metals, and oxidative potentials (Hao et al., 2020; B. Liu et al., 2017; Targino et al., 2016). In other words, $PM_{2.5}$ toxicity adjacent to different emission sources and land-use patterns may cause heterogeneous exposure risks to populations both near and far. Failure to consider the spatial heterogeneity of risks among urban and rural areas could lead to a potential bias of the BD estimations, and its uncertainty should be quantified.

Moreover, the data sources of $PM_{2.5}$ exposure concentration varied within studies and also contributed to the uncertainty of BD estimations. The straightforward method to estimate $PM_{2.5}$ exposure is to use measurements from the closest air quality monitoring sites, but using monitoring data alone to represent the whole region could bias short-term $PM_{2.5}$ exposure for the distant areas (McGuinn et al., 2017). In addition, using more sophisticated methods such as satellite data or air quality modeling data, which need further processing before application, can identify different $PM_{2.5}$ concentration in urban and rural areas, but failing to validate modeled results with observations in most studies can mean overlooking important deviations from reality and increasing uncertainties of BD estimation. Even though the difference of $PM_{2.5}$ exposure estimations between monitoring data, air quality modeled data, and satellite data had been identified (Garcia et al., 2016; McGuinn et al., 2017), the derived uncertainty for the BD calculations among urban and rural areas was still not further investigated. Nonetheless, except for the heterogeneous risks in urban and rural areas, the uncertainties between these $PM_{2.5}$ exposure assessment methods for the BD calculations need to be quantified as well.

This study applied the developed framework to Tainan City in Taiwan as a use case, estimated the risks of death, CVD, and RD by using 2006–2016 emergency department (ED) visit data, air quality monitoring data, and land-use characteristics, and further estimated the BD caused by daily $PM_{2.5}$ exposure in 2013. Our objectives are (1) to build up a data fusion framework to estimate the disease burden of daily $PM_{2.5}$ exposure while evaluating local risks and their spatial heterogeneities with hospital ED visit, land-use, emission, monitoring, modeling, and population data and (2) to quantify the spatial heterogeneity of risks and its relationship with land-use characteristics and derived uncertainty during BD calculation. This study systematically focused on the spatial heterogeneity of health risks at grid-level scale (1 km \times 1 km) and quantified method uncertainties of the BD estimations.

2. Material and methods

2.1. Data collection

2.1.1. Hospital emergency department (ED) visit data

Study subjects were extracted from the hourly hospital ED visit database (2006–2016) maintained by Chi Mei Hospital, a regional medical center located in Tainan City (Figure S1(a)). Patients with CVD ($N = 12,524$), RD ($N = 18,891$), and non-accidental death ($N = 37,846$) were selected based on the International Classification of Diseases, 9th edition (ICD-9) codes (CVD: heart failure (428), cardiac dysrhythmia (426–427), cerebrovascular disease (430–437), ischemic heart disease (410–414), peripheral vascular disease (440–449); RD: chronic obstructive pulmonary disease (490–492), respiratory tract infection (464–466, 480–487)). If the subject was admitted more than once during the same month, the earlier record was used. This study was approved by the Institutional Review Board of Chi-Mei Medical Center (No. 10612–012) and was exempt from obtaining informed consent.

2.1.2. Air quality and meteorological data

Subject exposure data were collected from the nearest air quality monitoring stations (AQMS) maintained by Taiwan Environmental Protection Administration (EPA) (Figure S1(a)). Hourly data of $PM_{2.5}$, PM_{10} (particulate matter $\leq 10 \mu m$ in aerodynamic diameter), nitrogen dioxide (NO_2), nitric oxide (NO), sulfur dioxide (SO_2), carbon monoxide (CO), ozone (O_3), ambient temperature, relative humidity, and wind speed were used for analysis. The arithmetical mean of the 24 hourly concentrations ($n = 24$, 1–24 h as an abbreviation) before the visit of each subject for each abovementioned pollutant and each abovementioned meteorological variable was calculated to represent the daily exposure of residents. Subjects with exposure to 1–24 h $PM_{2.5}$ mean concentration $\leq 25 \mu g/m^3$ before visit were excluded based on the daily $PM_{2.5}$ standard of the World Health Organization (WHO) (World Health Organization, 2005).

2.1.3. Emission data

Primary $PM_{2.5}$ emission data from Taiwan Emission Data System (TEDS) version 9.0 including industrial, mobile, area, and natural sources were utilized to evaluate the potential exposure of subjects to neighboring $PM_{2.5}$ emissions. $PM_{2.5}$ emission within a 1-km radius of the center of each grid cell was further summed up for analysis (Figure S1(b)).

2.1.4. Land-use data and population data

Land-use data of 2011 were acquired from National Land Survey and Mapping Center. A total of 2406 grid cells with 1 km \times 1 km horizontal resolution in Tainan City was created. Considering the daily living pattern of residents, nine ($k = 9$) land-use types were included to represent areas visited frequently by subjects. These land-use types included the high-density residential area (HDRA), low-density residential area (LDRA), agriculture (including livestock farming), industrial areas, retailing sites, recreation sites (including parks, recreation centers, and gyms), schools and education institutes, road areas, and undeveloped areas (including bare lands, forests, and water bodies). Population data of 2013 were obtained from the Department of Household Registration within the Ministry of the Interior and further spatially distributed by total residential area (HDRA and LDRA) of each grid cell.

2.1.5. Quantification of neighboring land-use characteristics

Land-use characteristics of areas neighboring subjects' typical living

activities were defined by neighboring PM_{2.5} emission and Heterogeneity of Land-Use Living (HLUL) patterns. The reason to use neighboring emission is that it can represent the level of primary PM_{2.5} to which subjects are potentially exposed, and it does not need complicated and time-consuming modeling procedure to simulate ambient PM_{2.5}. In addition, HLUL patterns reflect the daily activities and exposure patterns which can enhance physical health by daily activities but also increase the frequency and duration of PM_{2.5} exposure. The levels of HLUL patterns were quantified by Mean Entropy Index (MEI) for all grid cells. MEI adapted from the Entropy Index (EI) (Hess et al., 2001; Kockelman, 1997; Song et al., 2013) can represent the potential mobility of residents in an area. MEI varies between 0 and 1, where a value of 1 represents the highest diversity and heterogeneity in land-use, and considers the land-use types of neighboring grid cells by using the following equation (Kockelman, 1997).

$$MEI = - \sum_{x=1}^n \frac{\sum_{y=1}^k \frac{A_{xy} \cdot P_{xy} \cdot \ln(P_{xy})}{\ln(k)}}{n} \quad (1)$$

where n is the number of surrounding grid cells ($n = 8$) of the estimated grid cell. k is the number of the total used land-use types ($k = 9$). A_{xy} is the ratio of selected or surrounding grid cell to the area within a 1-km radius of each selected grid cell. P_{xy} is the proportion of land-use type y in the selected and surrounding x th grid cell.

2.2. Developed framework

Our data fusion framework is illustrated in Fig. 1. The number of ED visits was used to evaluate the BD, and the ED visits were calculated from short-term PM_{2.5} exposure risk, daily PM_{2.5} concentration, and population data (Davidson et al., 2007). First, the hospital ED visit data, air quality monitoring data, emission data, and land-use data were fused by case-crossover study design and stratified analysis to retrieve short-term (1–24 h) PM_{2.5} exposure risk and its spatial heterogeneity (Section 2.2.1). Technically, the overall short-term PM_{2.5} exposure risk was first assessed by case-crossover study design which involved hospital ED visit (Section 2.1.1) and air quality monitoring data (Section 2.1.2), and then stratified analysis was executed to assess the heterogeneous risks for subjects living in different land-use characteristics (Section 2.1.5).

Second, we used daily PM_{2.5} concentration data in 2013 as an example to illustrate the process to build up the BD map of CVD, RD, and death in 2013. The daily PM_{2.5} concentration data were extracted from the fused estimations of modeled results and monitoring data by Measurement-Model Fusion (MMF) approach (Zhang et al., 2019). The modeled results were firstly simulated by Community Multiscale Air Quality (CMAQ) (U.S. EPA Office of Research and Development, 2017) modeling and then fused with monitoring data from AQMS by applying the ratio of modeled PM_{2.5} to observed PM_{2.5} obtained from the nearest site (Section 2.2.2, equation (4)).

Overall, all parameters (PM_{2.5} exposure risk, daily PM_{2.5} concentration in 2013 and population) for calculating ED visits were resolved with 1 km × 1 km resolution and applied to build up the BD map in 2013 through CRFs (Section 2.2.3, equation (5)). Also, a sensitivity analysis was conducted to quantify the uncertainties of the BD estimations under different scenarios (Section 2.3).

2.2.1. Evaluating PM_{2.5} exposure risks and their spatial heterogeneity

We employed a case-crossover study design to investigate the relationship between 1 and 24 h PM_{2.5} exposure before the ED visit and health outcomes (Li et al., 2016; Yorifuji et al., 2014a, 2014b). Detailed descriptions can be found in our previous publication (Wu et al., 2020). Briefly, for each case, exposure before the visit is compared with exposure at the other control periods and the controls were selected from the same time of ED visits on the other days, on the same day of the week in the same month and year (Bhaskaran et al., 2013; Li et al., 2016; Yorifuji et al., 2014a, 2014b). Conditional logistic regressions were conducted to estimate adjusted odds ratios (ORs) and 95% confidence intervals (CIs) for the relationship between PM_{2.5} exposure and health outcomes. Our multi-pollutant model was described below:

$$\text{logitP}(Y_i) = \ln \left(\widehat{OR}_i \right) = \beta_0 + \beta_1 PM_{2.5i} + \beta_2 T_i + \beta_3 RH_i + \beta_4 WS_i + \beta_5 P_{il} + \dots + \beta_p P_{ip} \quad (2)$$

where $P(Y_i)$ is the natural logarithm of the OR for case subjects i compared with individual controls, and β_0 is the intercept. All predicting variables use 1–24 h mean before the visit of subjects. For example, $PM_{2.5i}$ is 1–24 h PM_{2.5} concentration before the visit of subjects i . $PM_{2.5ii}$,

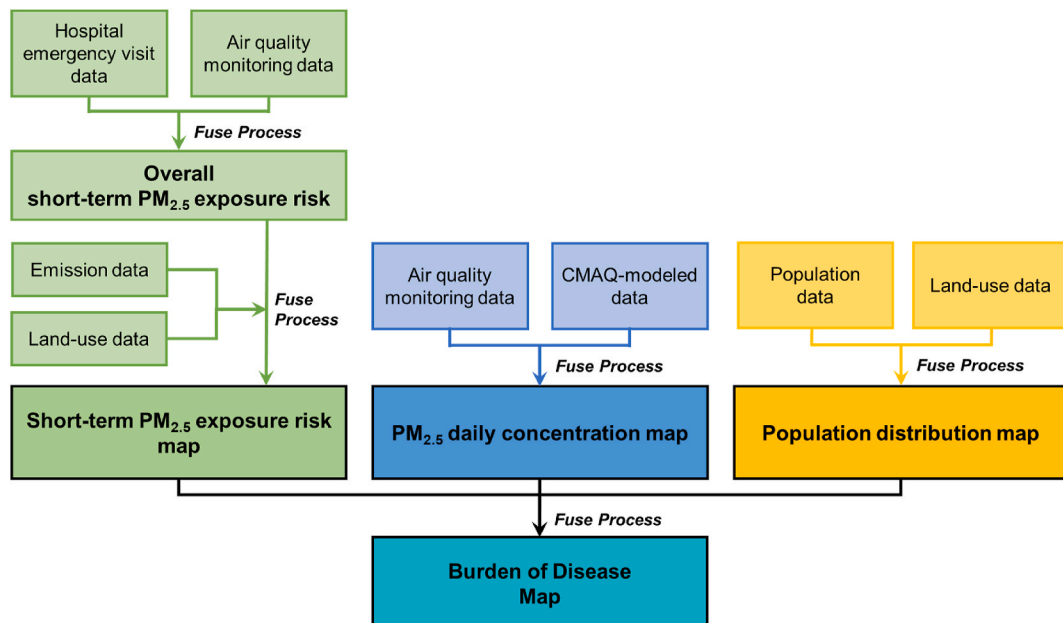


Fig. 1. Data structure of this study.

T_i (temperature), RH_i (relative humidity), and WS_i (wind speed) were included as fixed variables in the model. Linear correlation between 1 and 24 h $PM_{2.5}$ exposure and health outcomes were assumed based on previous findings (Linares and Díaz, 2010; Yorifuji et al., 2014a, 2014b). Natural cubic splines with three degrees of freedom (df) were used in all models to adjust the potential time-variant confounders including T_i , RH_i , and WS_i (Bhaskaran et al., 2013; Li et al., 2016; Rich et al., 2018). $P_{i1} \dots P_{ip}$ are the selected pollutants p which served as adjusting variables (covariates) and were chosen by stepwise selection. The significant level (p-value) for stepwise selection to keep or discard the variable was 0.05. For each health outcome, the final model was chosen to yield the minimum Akaike information criteria (AIC) statistic, and the collinearity of included variables was assessed by the variance inflation factor (VIF) (Table S1).

In advance, we performed the stratified analysis (Weichenthal et al., 2016) by applying the same model (equation (2)) to the subjects living in the different categories of land-use characteristics to assess the spatial heterogeneity of $PM_{2.5}$ exposure risk. First, we equally categorized the subjects of death, CVD, and RD by their indices (MEI and neighboring $PM_{2.5}$ emission, respectively) with low (<33rd percentile), medium (33rd - 66th percentile), and high (>66th percentile) level according to their residential address. Second, for each health outcome, multi-pollutant modeling (equation (2)) was first conducted to obtain the ORs for overall subjects, and the same model was then applied to the subjects of the low-, medium- and high-level groups for MEI and neighboring $PM_{2.5}$ emission, respectively. Third, the subjects were next grouped by MEI and $PM_{2.5}$ emission categories to assess the interaction of MEI and neighboring $PM_{2.5}$ emission to the health outcomes, and a total of nine groups (three by three categories) were assessed. The same model (equation (2)) for overall subjects was also applied for each group again, and the group-specific risk could be obtained. For each group, the specific risk was calculated as:

$$\widehat{OR}_{i,g} = \exp(\beta_0 + \beta_1 PM_{2.5,i,g} + \beta_2 T_{i,g} + \beta_3 RH_{i,g} + \beta_4 WS_{i,g} + \beta_5 P_{i1,g} + \dots + \beta_p P_{ip,g}) \quad (3)$$

where $\widehat{OR}_{i,g}$ was the risk of a group g from one to nine, and the other included parameters were the same as equation (2). By matching the group-specific risks with grid cells, the risk map can be built up.

2.2.2. Simulating $PM_{2.5}$ concentration

The daily $PM_{2.5}$ concentration data in 2013 were modeled by CMAQ with 3 km \times 3 km resolution and adjusted by using the monitoring data. The CMAQ modeling system was developed by the U.S. EPA and the user's community. CMAQ model can provide temporally and spatially varying air pollutant concentrations by calculating physical and chemical interactions between pollutants and meteorological factors in the atmosphere (U.S. EPA Office of Research and Development, 2017). The modeled daily $PM_{2.5}$ concentrations were further fused with monitoring data by the MMF method. For each grid cell at each day, the modeled daily $PM_{2.5}$ means were adjusted by the ratio of modeled $PM_{2.5}$ to observed $PM_{2.5}$ obtained from the nearest site (Zhang et al., 2019), which was calculated as:

$$Fused PM_{2.5,d,g} = \frac{Observed PM_{2.5,d,s}}{Modeled PM_{2.5,d,s}} \cdot Modeled PM_{2.5,d,g} \quad (4)$$

where Fused $PM_{2.5,d,g}$ and Modeled $PM_{2.5,d,g}$ is CMAQ-fused and CMAQ-modeled $PM_{2.5}$ in grid cell g at the d th day, respectively, and Observed $PM_{2.5,d,s}$ and Modeled $PM_{2.5,d,s}$ is observed and CMAQ-modeled $PM_{2.5}$ at the d th day for the monitoring site s which is closest to the grid cell g . The 3 km \times 3 km CMAQ-fused results were integrated with 1 km \times 1 km population data and each 1 km \times 1 km grid cell included the closest CMAQ-fused data to calculate the number of daily excess ED visits or deaths for each grid cell. Because illustrating the different vulnerabilities in urban and rural areas and derived

uncertainties from different sources are our objective, we only applied the basic MMF to fuse modeled data and monitoring data.

2.2.3. Estimating the BD of $PM_{2.5}$ exposure

The BD of $PM_{2.5}$ exposure was calculated by CRFs, which can quantify the increased ED visits due to daily $PM_{2.5}$ exposure in 2013 (Davidson et al., 2007). The number of ED visits for each grid cell was calculated by the following equation:

$$Y = E_0 \cdot P \cdot (1 - e^{-\beta \cdot (C - C_0)}) \cdot A \quad (5)$$

where Y is the number of daily excess ED visits or deaths caused by daily $PM_{2.5}$ exposure. E_0 is the actual morbidity or mortality rate. P is the population of each grid cell. The coefficient β is derived from RR, and RR is approximated by using OR obtained from equation (2) or (3) (Bhaskaran et al., 2013). A is a scalar of 1/365 to convert the annual rate to daily rate. C_0 is the threshold concentration set as the WHO $PM_{2.5}$ daily standard of 25 $\mu\text{g}/\text{m}^3$. C is the daily $PM_{2.5}$ concentration in each grid cell.

2.3. Uncertainty analysis

We considered the uncertainty of the BD (the number of daily excess ED visits or deaths) estimations mostly originated from the value of risk coefficient (β) and daily $PM_{2.5}$ concentration (C) in equation (5). Thus, we conducted a sensitivity analysis and compared the BD estimations from three nested scenarios, including (1) using non-local or local risk estimates to calculate the local BD. The non-local risk estimates were referred from the U.S. EPA recommended values in Environmental Benefits Mapping and Analysis Program - Community Edition (BenMAP-CE, version 1.1.3) software package (U.S. EPA, 2014), which can be treated as the literature-based risks from other countries and regions, because U.S. EPA recommended risks were also referred from multiple well-designed studies. The local risk estimates were obtained by the conditional logistic regression (equation (2)) among overall subjects; (2) using averaged risk or heterogeneously distributed risks to calculate the burdens. The heterogeneously distributed risks were obtained by stratified analysis (equation (3)) for different land-use characteristics; (3) using monitoring data from the nearest AQMS or CMAQ-fused data to represent daily $PM_{2.5}$ exposure. SAS statistical software (SAS 9.4; SAS Institute Inc., Cary, NC, USA) was used to perform all analytical procedures.

3. Results

3.1. Descriptive analysis

Descriptive analysis of subjects (Table S2) showed that the number of females comprising the BD was higher than that of males. More elderly subjects visited the ED with CVD, while more young subjects visited due to RD or death. All subjects with air-quality related health conditions visited the ED more frequently during the nighttime as compared with daytime. During the study period, the $PM_{2.5}$ mean concentration from four AQMSs in Tainan City was $25.12 \pm 17.95 \mu\text{g}/\text{m}^3$ (Table S3). For HLUL patterns, MEI was normally distributed with a mean \pm standard deviation of 0.350 ± 0.136 (unitless) (Figure S2 and Table S4). The spatial distribution of MEI in Fig. 2 showed that the most intensely heterogeneous areas (darker color) are located in the southern city, which consists of a mix of urban, suburban, and industrial-rural land-use types. Areas adjacent to the main roads also showed high heterogeneity. In contrast, the eastern areas of the city were less heterogeneous (lighter color) due to their mountainous terrain.

3.2. Heterogeneous risks associated with HLUL patterns and $PM_{2.5}$ emission

Estimated risks of 1–24 h $PM_{2.5}$ exposure (per 10 $\mu\text{g}/\text{m}^3$ increase) for

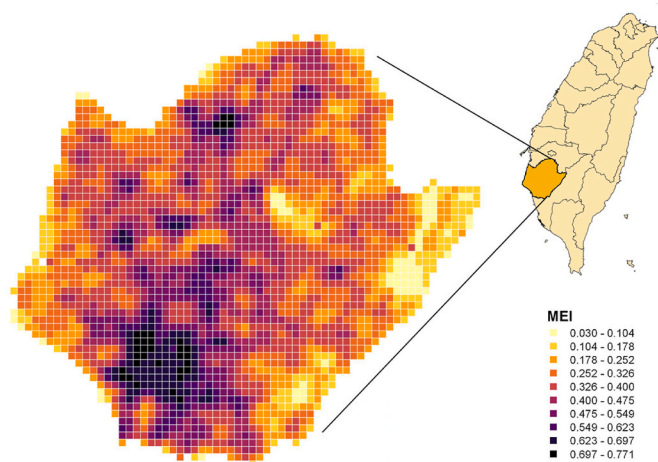


Fig. 2. MEI map of Tainan City with 1 km × 1 km resolution.

different levels of HLUL patterns are presented in Table S5 and Fig. 3(a). The average risk of CVD (OR = 1.27, 95% CI: 1.24–1.30) is the highest compared with RD (OR = 1.26, 95% CI: 1.23–1.29) and non-accidental death (OR = 1.25, 95% CI: 1.22–1.27) (Table S5). The risks of PM_{2.5}

exposure also varied with the levels of HLUL patterns. For CVD and RD, the risk increased with the increase in HLUL patterns, and high HLUL patterns increased risk up to 59% (OR = 1.59, 95% CI: 1.46–1.73) and 36% (OR = 1.36, 95% CI: 1.29–1.45), respectively. On the contrary, low-level HLUL patterns were correlated with a higher risk of death (OR = 1.31, 95% CI: 1.25–1.37).

Regarding neighboring PM_{2.5} emission (Table S5 and Fig. 3(b)), subjects in proximity to the medium level of PM_{2.5} emission had the highest risk for all selected BD outcomes. The highest risks for CVD, death, and RD were identified in subjects adjacent to the medium-level PM_{2.5} emission, for which ORs were 1.52 (95% CI: 1.40–1.66), 1.51 (95% CI: 1.41–1.61), and 1.47 (95% CI: 1.38–1.57), respectively. Furthermore, the reduced risk of death was observed for subjects in proximity to high-level PM_{2.5} emission (OR = 0.95, 95% CI: 0.89–1.01), although results were not statistically significant.

3.3. Risk mapping building

The risk estimations from different combinations of HLUL pattern levels and PM_{2.5} emission categories by applying stratified analysis are shown in Table S6. Generally, higher risks are observed for subjects in high HLUL pattern areas and proximity to a medium-level PM_{2.5} emission, and the highest risk is observed for CVD (OR = 1.99, 95% CI: 1.50–2.64), followed by death (OR = 1.74, 95% CI: 1.47–2.07), and RD

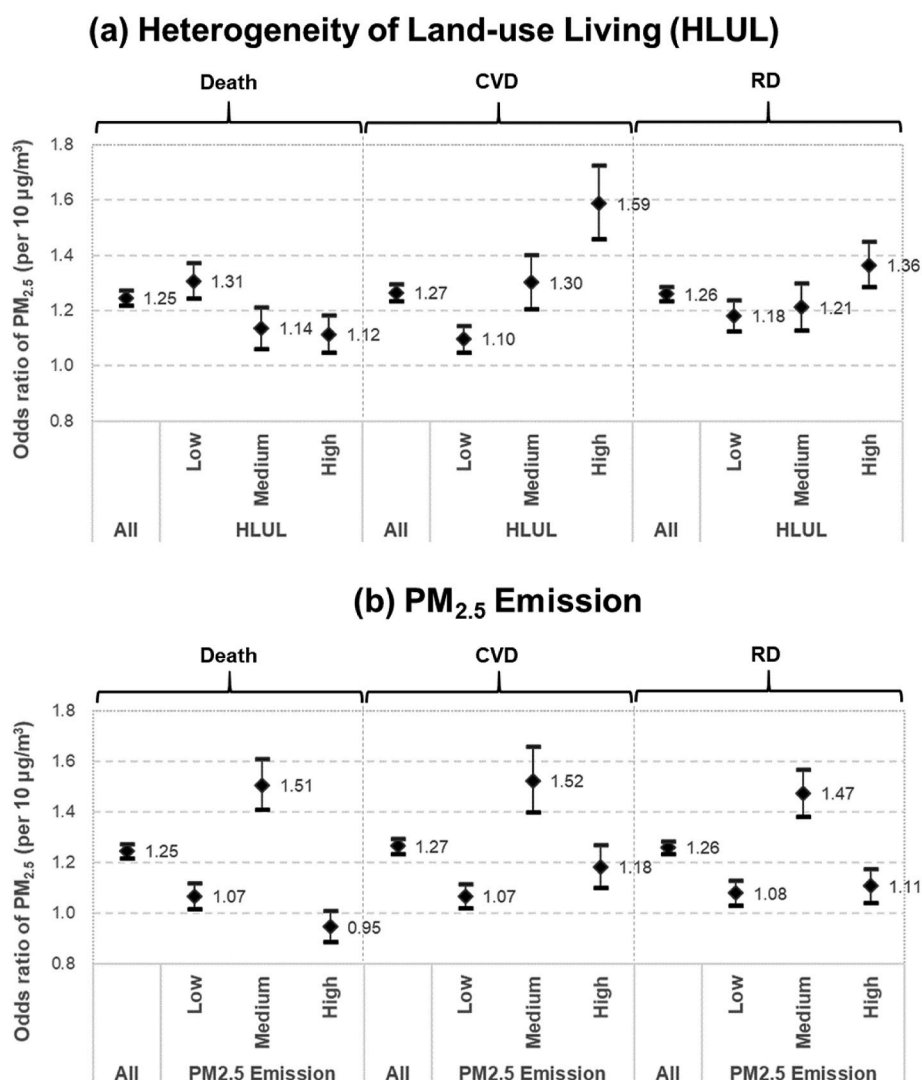


Fig. 3. Adjusted ORs and 95% CIs per 10 µg/m³ increase of PM_{2.5} for different levels of neighboring (a) HLUL patterns and (b) PM_{2.5} emission.

(OR = 1.52, 95% CI: 1.32–1.74). In addition, significantly reduced risks (OR < 1) are also observed in death subjects with low emission/medium HLUL pattern, medium emission/low HLUL pattern, and high emission/high HLUL pattern combinations.

The risk map of death (Fig. 4(a)) illustrates that the risk of death in rural areas was 1.40 times higher than average, while the risks of CVD and RD (Fig. 4(b) and (c)) in the most urbanized areas were 1.57 and 1.20 times higher than average. The spatial heterogeneity of risks implies that even though the residents have similar PM_{2.5} exposure, those who lived in areas with diverse land-use characteristics would have different vulnerabilities to PM_{2.5} exposure. Based on the identified linkage between PM_{2.5} exposure risk and land-use characteristics, we considered this spatial heterogeneity of the vulnerability could be associated with land-use characteristics in our study region. Also, the separately quantified risks for each health outcome have similar spatial patterns, which indicates that the correlation between land-use patterns and vulnerability could exhibit a generalizable trend. Residents in the most urbanized areas have a higher vulnerability to PM_{2.5} exposure for CVD and RD; residents living along main roads and highways are also less vulnerable to death and RD. In addition, residents in rural areas are at higher risk of death due to PM_{2.5} exposure. While similar previous studies have ignored the land-use related heterogeneity of PM_{2.5} exposure vulnerabilities and focused more on air pollutant concentrations, our results pointed out that subject vulnerability could potentially vary with the land-use characteristics of their activity spheres and those that neighbor them, and the spatial heterogeneity of those land-use characteristics and vulnerability could affect BD estimations.

4. Discussion

4.1. Risk of short-term PM_{2.5} exposure

The ORs of non-accidental death, CVD, and RD for 1–24 h PM_{2.5} exposure before the visit in this study were 1.25, 1.27, and 1.26, respectively, which are higher than those of previous studies conducted in the other developed or developing countries/regions (Table S7–9). Since the developed framework utilized local databases, it is not surprising that there is a potential difference between local risk estimations and risks from other regions or counties due to different environmental, demographic, and societal characteristics. This significant difference also implies the potential risk of using non-local risk values such as U.S. EPA recommended or literature-based risks for BD calculation.

One explanation for our higher OR estimations could be that the composition of PM_{2.5} in the study region was more toxic than that of PM_{2.5} measured in other countries or regions. For example, long-range transboundary air pollution transported from mainland China, which

contains a higher hazardous composition of PM_{2.5} and by-products of combustion (e.g. sulfate), exacerbates the health impact (S.T. Liu et al., 2017; Tsai et al., 2012). The risk of exposure to PM_{2.5} could be also amplified by the coexistence of NO₂ and O₃ in urban areas (Weichenthal et al., 2016). In this study, the significant correlation between daily PM_{2.5} and daily NO₂ (Pearson's $r = 0.57$, p -value < 0.01) and O₃ (Pearson's $r = 0.30$, p -value < 0.01) magnified the health impact of PM_{2.5} exposure. In addition, selection bias could also have contributed to the higher estimations. Because the subjects were selected from cases in the hospital and used as controls as well, the higher risk may have been due to subjects having been relatively more vulnerable to PM_{2.5} exposure compared with the general population. Furthermore, the full-coverage and complete national health insurance among all residents and lower medical expense in Taiwan may also increase the willingness of people to visit the ED even they have non-fatal diseases or symptoms. We also conducted extra sensitivity analyses to exclude the possible bias from modeling (Appendix A1), and the results proved the robustness of the model.

4.2. Risk of high HLUL patterns and neighboring to a medium-level PM_{2.5} emission

The CVD and RD risks due to PM_{2.5} exposure increased for subjects living in high HLUL patterns and neighboring to a medium-level PM_{2.5} emission. If both high HLUL patterns and a medium-level PM_{2.5} emission occurred simultaneously, the risk increased considerably. The increased risks of living in high HLUL patterns could be related to mixed land-use patterns. Residential areas neighboring high-emission areas like industrial areas or roads have shown higher risks of health impacts from air quality (Cambra et al., 2011; Ebisu et al., 2011; Son et al., 2015). In addition, subjects close to a medium-level PM_{2.5} emission suffered comparable risks which are higher than proximity to a higher-level PM_{2.5} emission. One explanation could be that the majority of PM_{2.5} mass concentration does not only originate from local regions. Secondary PM_{2.5} transported from other up-wind polluted regions may lead to subjects in these areas underestimating their exposure and reducing their awareness of air pollution. Previous studies in Taiwan found that secondary aerosol could contribute 25–60% of total PM_{2.5} mass, including 8–27% of total PM_{2.5} mass transported from mainland China and coastal cities in Taiwan (Hsu et al., 2017; Kuo et al., 2014; Liao et al., 2015; Lu et al., 2016).

4.3. Heterogeneous vulnerability in urban, suburban, and rural areas

Fig. 4 showed that the highest risks were 1.20–1.57 times higher than the average risks, especially in highly urbanized and rural areas. The

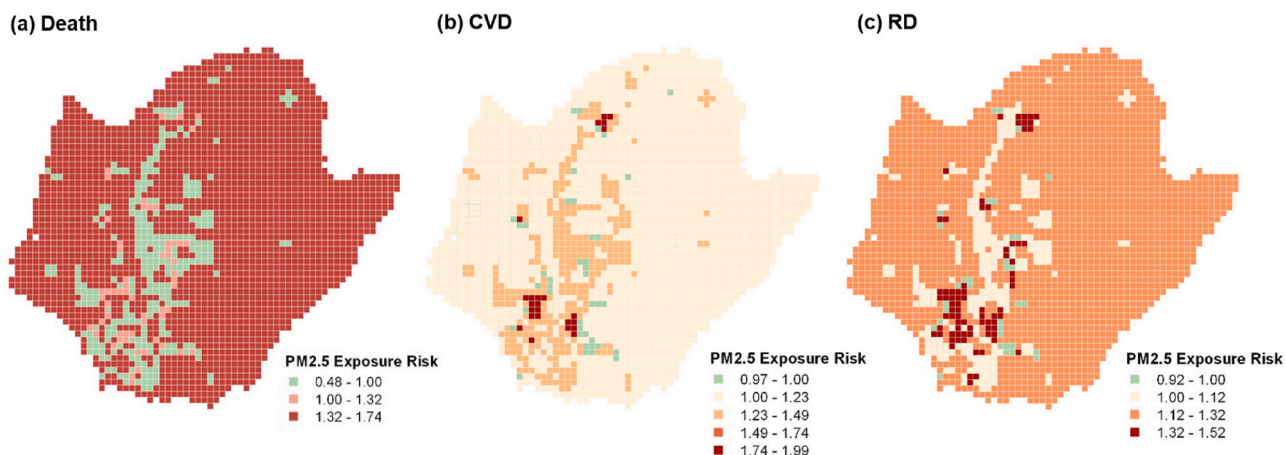


Fig. 4. Risk map of PM_{2.5} (per 10 µg/m³ increase) for (a) death, (b) CVD and (c) RD in Tainan City.

Table 1
Number of increased ED visits under different scenarios in Tainan City (2013)

Scenario	Applied OR of daily PM _{2.5} concentration (per 10 µg/m ³)	N (%) ^a		
		Monitoring data	CMAQ-Fused data	Difference ^b
<u>Death</u>				
Gridded Local Risk	1.000 ^c - 1.742	1699 (100%)	2137 (100%)	-437 (-20%)
Averaged Local Risk	1.245	1698 (100%)	2266 (106%)	-568 (-25%)
U.S. EPA Recommended Risk	1.170 ^d	1309 (77%)	1790 (84%)	-481 (-27%)
<u>CVD</u>				
Gridded Local Risk	1.000 ^c - 1.992	1297 (100%)	1750 (100%)	-453 (-26%)
Averaged Local Risk	1.266	1790 (138%)	2375 (136%)	-585 (-25%)
U. S. EPA Recommended Risk	1.002 ^d	178 (14%)	262 (15%)	-85 (-32%)
<u>RD</u>				
Gridded Local Risk	1.000 ^c - 1.518	1339 (100%)	1782 (100%)	-443 (-25%)
Averaged Local Risk	1.260	1763 (132%)	2343 (132%)	-580 (-25%)
U.S. EPA Recommended Risk	1.002 ^d	241 (18%)	355 (20%)	-113 (-32%)

^a The percentage present the portion of ED visits divided by ED visits of gridded local risk scenario.

^b Number of Monitoring data– Number of Fused data (% divided by fused estimation).

^c Grids with OR<1 were replaced by OR = 1 to assure non-negative number of ED visits.

^d For each health outcome, the highest risk was used from U.S. EPA recommended risk in BenMAP-CE (Version 1.1.3), <http://www.epa.gov/air/benmap>.

disparate risks among rural and urban areas might be due to the factors including human-environment interactions, individual factors, and PM_{2.5} toxicity. First, concerning individual factors, one reason for the higher vulnerability in rural areas is lower accessibility of medical resources, which is attributable to longer distances to hospitals; lower the abundance of medical professionals and reduced willingness to seek medical services (De-Miguel-Balsa et al., 2015; Simões and Almeida, 2011). Garcia et al. (2016) and Kloog et al. (2014) attributed these disparities to a “non-metropolitan penalty”, which refers to the difference in individual-level behaviors, medical accessibility, and the level of knowledge of diseases and their prevention. Second, the interaction between humans and their environment such as daily living pattern and exposure intensity, duration, and frequency could affect the level of the risk. Subjects in rural areas could have higher exposure frequency and longer exposure duration due to daily commuting and other outdoor activities (Chuang et al., 2020). Third, the difference in chemical and physical compositions between rural and urban PM_{2.5} could contribute to the risk difference. Higher risks of CVD and RD in more urbanized areas could be related to higher emissions from mobile and commercial sources (e.g. restaurants, street vendors) at breathing level (Du et al., 2016). Additionally, it should be noted that although residing in urban areas was found to enhance the risks of CVD and RD, the risk of death in rural areas was still higher than in urban areas, which suggests that the protective factors like high transportation and medical accessibility in the urban and suburban environments could lower the risk of death, and residents in rural areas could have a lower willingness and lack of medical resources to receive medical treatment in time to prevent death.

In addition, reduced risk of PM_{2.5} exposure for death was observed in suburban areas (Fig. 4(a)), which could be associated with higher awareness of air pollution for residents in suburban areas. This finding is similar to that of Chan and Ng (2011), who speculated that vulnerable groups might be more aware of PM_{2.5} events and reduce their outdoor activities. Eberhardt and Pamuk (2004) also found that the health status of suburban area residents was superior to those living in both the most rural and the most urban areas.

4.4. Uncertainty quantification

Concerning estimation uncertainties, we considered that the bias could originate from the following scenarios: (1) using non-local estimated risk for calculating the local BD, (2) using averaged risk to represent the whole study region without considering population distribution and heterogeneously distributed risks, and (3) using monitoring data to represent ambient PM_{2.5} concentration among large regions including areas far from the AQMS. Thus, we designed six scenarios using three sources of risk values and two sources of PM_{2.5}

exposure data as shown in Table 1, including the estimated ED visits and the uncertainties between scenarios. Descriptive analysis of observed and CMAQ-fused PM_{2.5} data are presented in Table S10. The validation of CMAQ-modeled results is shown in Table S11. The spatial distribution of the annual mean of CMAQ-fused PM_{2.5} is shown in Figure S3. CMAQ-modeled results for all sites in this study region meet both of the performance criteria of Taiwan EPA and U.S. EPA (U.S. EPA, 2007).

First, risks using estimated data, based on U.S. EPA recommended values, contributed the greatest uncertainty to the results as it underestimated the local ED visits by 16–86% compared with using gridded local risks. This high uncertainty also emphasized the potential bias when using U.S. EPA recommended values or literature-based risk estimates from other countries or regions to calculate the local BD. In this study, if local gridded risk estimates were used in our study region, the estimated ED visits increased substantially by 1.19–7.29 times.

Moreover, when using monitoring data to calculate the BD, the results were lower than using CMAQ-fused data, primarily because using monitoring data could have a bias in distant areas far from the monitoring site. Therefore, using monitoring data to represent distant areas resulted in the underestimation of ED visits by 20–32% in our study region. Although uncertainties occasionally exhibited in the monitoring data, it was still useful in the study due to higher availability and shorter time to model execution. Additionally, while using CMAQ-fused data is a more appropriate method to represent exposure more accurately for subjects in distant areas where measurements are not directly available, the modeling results still need to be validated and require more time and resources to execute. Both techniques have advantages and disadvantages, and for calculating the BD, we quantified the estimation uncertainties between these two methods to be 20–32%.

Additionally, concerning the spatial heterogeneity of risk, when using gridded risks other than averaged risks, the number of ED visits is decreased by 0–38%. This is because the disaggregated calculation considered the distribution of population and their specific risks in urban, suburban, and rural areas. Figure S4 shows the spatial difference between these two scenarios, where red and blue grid cells represent the overestimation and underestimation, respectively, of the averaged-risk method compared with the gridded-risk method. Using averaged risks underestimates the ED visits in urban areas for all outcomes, and overestimates risk in suburban areas for death, rural areas for CVD, and suburban and rural areas for RD.

Overall, concerning uncertainty from risk values and daily PM_{2.5} concentration, using non-local risk estimates has the largest uncertainty (16–86%), followed by using monitoring data (20–32%) and applying the same averaged risks to represent the vulnerability of the population in rural and urban areas (0–38%), especially in most urbanized areas. The most biased estimation using non-local risk estimates and

monitoring data underestimates the BD by 39–90% compared with using heterogeneously distributed local risks estimates and CMAQ-fused data. Thus, previous studies using nation-wide risk to estimate the BD or cost-benefit of air quality implementation could be potentially biased, because they overlooked the distribution of populations and their heterogeneous risks in areas with diverse levels of urbanization, and these risks could vary within a wide range (e.g. OR of death could be 39% higher than the average) (Burnett et al., 2014; Chen et al., 2017; GBD, 2017 Risk Factor Collaborators, 2018). When ignoring the spatial heterogeneity of risk, the effectiveness of air quality control implementation could be limited and remain biased.

4.5. The strengths of our framework

Our framework to calculate the BD has several advantages over previous calculations. First, our framework can provide cities or countries with a framework to develop their own BD estimations by using local databases, since the uncertainties arising from lack of available administrative health data in smaller regions, cities, and communities have been gradually come to be recognized (GBD, 2017 Risk Factor Collaborators, 2018). For those regions or countries without local land-use or emission data, using satellite data can provide an alternative way to build up a local land-use database (Talukdar et al., 2020), while emission data could be obtained from local government or a global emission database such as ECLIPSE that has been widely used for many international studies (Stohl et al., 2015) and can be spatially distributed by population density, road lengths, or other anthropogenic indices. Once regions or countries have the required databases, our developed framework can be applied in any location. Second, the risk map can identify the spatial heterogeneity of risks and identify areas with higher risks. Combined with the BD map, the maps can facilitate the allocation of public and medical resources by local governments to affected areas and reduce potential health impacts more effectively. For example, in this study, we identified lower risks of CVD and RD but a higher risk of death in rural areas, and we suggested that one of the explanations for this tendency is the lower accessibility of residents in these areas to medical medical treatment and/or the lower willingness of residents to accept treatment. Third, with prior information about the spatial distribution of PM_{2.5} exposure risk, the health officials can more accurately estimate the number of potential ED visits based on timely air pollution forecasts, so that medical and emergency care systems can be better prepared for surges in emergency department care demand.

4.6. Limitations

Our study still has some limitations. First, our framework only partially captures individual-level exposure patterns. For instance, although we located subjects by their residential address, it is possible that these subjects travel to another area for school or work. During working or staying indoors, the variation in the intensity of individual-level exposure could also confound the impact of ambient PM_{2.5}. One potential strategy for solving this problem is collecting time-activity data, which would allow the duration of outdoor and indoor activities for individuals or groups to be used to classify exposure level, but this method is time-consuming, costly, and its representativeness is easily limited by sample size and sampling methods. Second, we only applied the basic MMF techniques to fuse modeled data and monitoring data. Advanced MMF techniques like machine learning techniques should be developed and tested in future work. Third, although we only applied the framework in one city, the impact of land-use characteristics on PM_{2.5} exposure risk could still generally exist in the developing countries. The identified relationship between land-use characteristics and PM_{2.5} exposure risk in this study region may be different from that in other regions or countries. Thus, more cities and regions need to be considered in future works when the hospital data become available.

5. Conclusion

The finer spatial resolution of risk and BD estimations are increasingly required for regional air quality and public health management. This study built up a data fusion framework that facilitates individual development of risk and BD estimates for cities or countries based on spatial heterogeneity among different land-use characteristics and urbanization levels to enhance the accuracy of the BD estimations. In this study, we discovered that living in areas with high HLUL patterns increases the risk of CVD and RD by 59% and 35%, and that living in areas with low HLUL patterns increases the risk of death by 31%. Residents in rural areas had 1.40 times higher death risk compared with the average risk, and residents in the most urbanized areas had 1.57 and 1.20 times higher risk of CVD and RD than average. Our developed framework provides the exposure risk maps and BD map at the grid-level resolution, that visualize these risks and the BD. Such illustrations facilitate reassessment of the potential risk of present urban planning strategies and provide a quantified reference for air quality implementation plans and emergency episode-response plans.

Declaration of competing interest

The authors declare that they have no known competing financial interests or personal relationships that could have appeared to influence the work reported in this paper.

Acknowledgements

The authors are grateful to Dr. Melissa Allen-Dumas at Oak Ridge National Laboratory and Matthew Tipton from the Department of Civil and Environmental Engineering, the University of Tennessee Knoxville for providing writing suggestions and revision. This study was supported by the grants from Chi-Mei Medical Center (CMFHR10752, 2018) and Taiwan EPA (EPA-106-FA18-03-A260, 2017). The funders had no role in study design, data collection and analysis, decision to publish, or preparation of the manuscript.

Appendix A. Supplementary data

Supplementary data to this article can be found online.

Appendix B. Supplementary data

Supplementary data to this article can be found online at <https://doi.org/10.1016/j.envpol.2021.117266>.

Credit author statement

Cheng-Pin Kuo: Writing – original draft, Writing – review & editing. Joshua S. Fu: Writing – original draft, Writing – review & editing, Supervision. Pei-Chih Wu: Hospital data providing and QA/QC. Tain-Junn Cheng: Hospital data providing and QA/QC. Tsu-Yun Chiu: Hospital data providing and QA/QC. Chun-Sheng Huang: Land-use and emission data providing and QA/QC. Chang-Fu Wu: Land-use and emission data providing and QA/QC. Li-Wei Lai: Air quality modeled and monitored data providing and QA/QC. Hsin-Chih Lai: Air quality modeled and monitored data providing and QA/QC. Cio-Kai Liang: Air quality modeled and monitored data providing and QA/QC.

References

- Apte, J.S., Brauer, M., Cohen, A.J., Ezzati, M., Pope, C.A., 2018. Ambient PM_{2.5} reduces global and regional life expectancy. *Environ. Sci. Technol. Lett.* 5, 546–551. <https://doi.org/10.1021/acs.estlett.8b00360>.
- Apte, J.S., Marshall, J.D., Cohen, A.J., Brauer, M., 2015. Addressing global mortality from ambient PM_{2.5}. *Environ. Sci. Technol.* 49, 8057–8066. <https://doi.org/10.1021/acs.est.5b01236>.

- Barton, H., 2009. Land use planning and health and well-being. *Land Use Pol.* 26, 115–123. <https://doi.org/10.1016/j.landusepol.2009.09.008>.
- Bhaskaran, K., Armstrong, B., Hajat, S., Haines, A., Wilkinson, P., Smeeth, L., 2013. Heat and risk of myocardial infarction: hourly level case-crossover analysis of MINAP database. *BMJ* 346, 1–14. <https://doi.org/10.1136/bmj.e8050>.
- Burnett, R.T., Arden Pope, C., Ezzati, M., Olives, C., Lim, S.S., Mehta, S., Shin, H.H., Singh, G., Hubbell, B., Brauer, M., Ross Anderson, H., Smith, K.R., Balmes, J.R., Bruce, N.G., Kan, H., Laden, F., Prüss-Ustün, A., Turner, M.C., Gapstur, S.M., Diver, W.R., Cohen, A., 2014. An integrated risk function for estimating the global burden of disease attributable to ambient fine particulate matter exposure. *Environ. Health Perspect.* 122, 397–403. <https://doi.org/10.1289/ehp.1307049>.
- Cambra, K., Martínez-Rueda, T., Alonso-Fustel, E., Cirarda, F.B., Ibáñez, B., Esnaola, S., Calvo, M., Aldasoro, E., Montoya, I., 2011. Mortality in small geographical areas and proximity to air polluting industries in the Basque Country (Spain). *Occup. Environ. Med.* 68, 140–147. <https://doi.org/10.1136/oem.2009.048215>.
- Chan, C.C., Ng, H.C., 2011. A case-crossover analysis of Asian dust storms and mortality in the downwind areas using 14-year data in Taipei. *Sci. Total Environ.* 410, 47–52. <https://doi.org/10.1016/j.scitotenv.2011.09.031>.
- Chen, L., Shi, M., Gao, S., Li, S., Mao, J., Zhang, H., Sun, Y., Bai, Z., Wang, Z., 2017. Assessment of population exposure to PM_{2.5} for mortality in China and its public health benefit based on BenMAP. *Environ. Pollut.* 221, 311–317. <https://doi.org/10.1016/j.envpol.2016.11.080>.
- Chuang, K.J., Lin, L.Y., Ho, K.F., Su, C.T., 2020. Traffic-related PM_{2.5} exposure and its cardiovascular effects among healthy commuters in Taipei, Taiwan. *Atmos. Environ.* X 7, 100084. <https://doi.org/10.1016/j.aesaa.2020.100084>.
- Davidson, K., Hallberg, A., McCubbin, D., Hubbell, B., 2007. Analysis of PM_{2.5} using the environmental benefits mapping and analysis program (BenMAP). *J. Toxicol. Environ. Health Part A Curr. Issues* 70, 332–346. <https://doi.org/10.1080/15287390600884982>.
- De-Miguel-Balsa, E., Latour-Pérez, J., Baeza-Román, A., Llamas-Álvarez, A., Ruiz-Ruiz, J., Fuset-Cabanes, M.P., 2015. Accessibility to reperfusion therapy among women with acute myocardial infarction: impact on hospital mortality. *J. Wom. Health* 24, 882–888. <https://doi.org/10.1089/jwh.2014.5011>.
- Ding, D., Zhu, Y., Jang, C., Lin, C., Wang, S., Fu, J., Gao, J., Deng, S., Xie, J., Qiu, X., 2016. Evaluation of health benefit using BenMAP-CE with an integrated scheme of model and monitor data during Guangzhou Asian Games. *J. Environ. Sci.* 42, 9–18. <https://doi.org/10.1016/j.jes.2015.06.003>.
- Du, Y., Xu, X., Chu, M., Guo, Y., Wang, J., 2016. Air particulate matter and cardiovascular disease: the epidemiological, biomedical and clinical evidence. *J. Thorac. Dis.* 8, E8–E19. <https://doi.org/10.3978/j.issn.2072-1439.2015.11.37>.
- Eberhardt, M.S., Pamuk, E.R., 2004. The importance of place of residence: examining health in rural and nonrural areas. *Am. J. Publ. Health* 94, 1682–1686. <https://doi.org/10.2105/AJPH.94.10.1682>.
- Ebisu, K., Holford, T.R., Belanger, K.D., Leaderer, B.P., Bell, M.L., 2011. Urban land-use and respiratory symptoms in infants. *Environ. Res.* 111, 677–684. <https://doi.org/10.1016/j.envres.2011.04.004>.
- Garcia, C.A., Yap, P.S., Park, H.Y., Weller, B.L., 2016. Association of long-term PM_{2.5} exposure with mortality using different air pollution exposure models: impacts in rural and urban California. *Int. J. Environ. Health Res.* 26, 145–157. <https://doi.org/10.1080/09603123.2015.1061113>.
- GBD 2017 Risk Factor Collaborators, 2018. Global, regional, and national comparative risk assessment of 84 behavioural, environmental and occupational, and metabolic risks or clusters of risks for 195 countries and territories, 1990–2017: a systematic analysis for the Global Burden of Disease Study. *Lancet* 392, 1923–1994. [https://doi.org/10.1016/S0140-6736\(18\)32225-6](https://doi.org/10.1016/S0140-6736(18)32225-6).
- Hao, Y., Meng, X., Yu, X., Lei, M., Li, W., Yang, W., Shi, F., Xie, S., 2020. Quantification of primary and secondary sources to PM_{2.5} using an improved source regional apportionment method in an industrial city. *China. Sci. Total Environ.* 706, 135715. <https://doi.org/10.1016/j.scitotenv.2019.135715>.
- Hess, P.M., Moudon, A.V., Logsdon, M.G., 2001. Measuring land use patterns for transportation research. *Transport. Res. Rec.* 17–24. <https://doi.org/10.3141/1780-03>.
- Hsu, C.Y., Chiang, H.C., Chen, M.J., Chuang, C.Y., Tsen, C.M., Fang, G.C., Tsai, Y.L., Chen, N.T., Lin, T.Y., Lin, S.L., Chen, Y.C., 2017. Ambient PM_{2.5} in the residential area near industrial complexes: spatiotemporal variation, source apportionment, and health impact. *Sci. Total Environ.* 590, 204–214. <https://doi.org/10.1016/j.scitotenv.2017.02.212>.
- Kloog, I., Nordio, F., Zanobetti, A., Coull, B.A., Koutrakis, P., Schwartz, J.D., 2014. Short term effects of particle exposure on hospital admissions in the mid-atlantic states: a population estimate. *PLoS One* 9, 1–7. <https://doi.org/10.1371/journal.pone.0088578>.
- Kockelman, K.M., 1997. Travel behavior as function of accessibility, land use mixing, and land use balance: evidence from San Francisco Bay Area. *Transport. Res. Rec.* 116–125. <https://doi.org/10.3141/1607-16>.
- Kuo, C.P., Liao, H.T., Chou, C.C.K., Wu, C.F., 2014. Source apportionment of particulate matter and selected volatile organic compounds with multiple time resolution data. *Sci. Total Environ.* 472, 880–887. <https://doi.org/10.1016/j.scitotenv.2013.11.114>.
- Li, S., Guo, Y., Williams, G., 2016. Acute impact of hourly ambient air pollution on preterm birth. *Environ. Health Perspect.* 124, 1623–1629. <https://doi.org/10.1289/EHP200>.
- Liao, H.T., Chou, C.C.K., Chow, J.C., Watson, J.G., Hopke, P.K., Wu, C.F., 2015. Source and risk apportionment of selected VOCs and PM_{2.5} species using partially constrained receptor models with multiple time resolution data. *Environ. Pollut.* 205, 121–130. <https://doi.org/10.1016/j.envpol.2015.05.035>.
- Linares, C., Díaz, J., 2010. Short-term effect of concentrations of fine particulate matter on hospital admissions due to cardiovascular and respiratory causes among the over-75 age group in Madrid, Spain. *Publ. Health* 124, 28–36. <https://doi.org/10.1016/j.puhe.2009.11.007>.
- Liu, B., Wu, J., Zhang, J., Wang, L., Yang, J., Liang, D., Dai, Q., Bi, X., Feng, Y., Zhang, Y., Zhang, Q., 2017. Characterization and source apportionment of PM_{2.5} based on error estimation from EPA PMF 5.0 model at a medium city in China. *Environ. Pollut.* 222, 10–22. <https://doi.org/10.1016/j.envpol.2017.01.005>.
- Liu, S.T., Liao, C.Y., Kuo, C.Y., Kuo, H.W., 2017. The effects of PM_{2.5} from asian dust storms on emergency room visits for cardiovascular and respiratory diseases. *Int. J. Environ. Res. Publ. Health* 14, 1–10. <https://doi.org/10.3390/ijerph14040428>.
- Lu, H.Y., Lin, S.L., Mwangi, J.K., Wang, L.C., Lin, H.Y., 2016. Characteristics and source apportionment of atmospheric PM_{2.5} at a coastal city in Southern Taiwan. *Aerosol Air Qual. Res.* 16, 1022–1034. <https://doi.org/10.4209/aaqr.2016.01.0008>.
- McGuinn, L.A., Ward-Caviness, C., Neas, L.M., Schneider, A., Di, Q., Chudnovsky, A., Schwartz, J., Koutrakis, P., Russell, A.G., Garcia, V., Kraus, W.E., Hauser, E.R., Cascio, W., Diaz-Sanchez, D., Devlin, R.B., 2017. Fine particulate matter and cardiovascular disease: comparison of assessment methods for long-term exposure. *Environ. Res.* 159, 16–23. <https://doi.org/10.1016/j.envres.2017.07.041>.
- Qiu, X., Zhu, Y., Jang, C., Lin, C., Wang, S., Fu, J., Xie, J., Wang, J., Ding, D., Long, S., 2015. Development of an Integrated Policy Making Tool for Assessing Air Quality and Human Health Bene Fi Ts of Air Pollution Control, vol. 9, pp. 1056–1065. <https://doi.org/10.1007/s11783-015-0796-8>.
- Rich, D.Q., Utell, M.J., Croft, D.P., Thurston, S.W., Thevenet-Morrison, K., Evans, K.A., Ling, F.S., Tian, Y., Hopke, P.K., 2018. Daily land use regression estimated woodsmoke and traffic pollution concentrations and the triggering of ST-elevation myocardial infarction: a case-crossover study. *Air Qual. Atmos. Heal.* 11, 239–244. <https://doi.org/10.1007/s11869-017-0537-1>.
- Simões, P.P., Almeida, R.M.V.R., 2011. Geographic accessibility to obstetric care and maternal mortality in a large metropolitan area of Brazil. *Int. J. Gynecol. Obstet.* 112, 25–29. <https://doi.org/10.1016/j.ijgo.2010.07.031>.
- Son, J.Y., Kim, H., Bell, M.L., 2015. Does urban land-use increase risk of asthma symptoms? *Environ. Res.* 142, 309–318. <https://doi.org/10.1016/j.envres.2015.06.042>.
- Song, Y., Merlin, L., Rodriguez, D., 2013. Comparing measures of urban land use mix. *Comput. Environ. Urban Syst.* 42, 1–13. <https://doi.org/10.1016/j.compenvurbysys.2013.08.001>.
- Stohl, A., Aamaas, B., Amann, M., Baker, L.H., Bellouin, N., Bernsten, T.K., Boucher, O., Cherian, R., Collins, W., Daskalakis, N., Dzusinska, M., Eckhardt, S., Fuglestad, J.S., Harju, M., Heyes, C., Hodnebrog, H., Im, U., Kanakidou, M., Klimont, Z., Kupiainen, K., Law, K.S., Lund, M.T., Maas, R., MacIntosh, C.R., Myhre, G., Myrriekelakakis, S., Olivie, D., Quaas, J., Quennehen, B., Raut, J.C., Rumbold, S.T., Samset, B.H., Schulz, M., Seland Shine, K.P., Skeie, R.B., Wang, S., Yttri, K.E., Zhu, T., 2015. Evaluating the climate and air quality impacts of short-lived pollutants. *Atmos. Chem. Phys.* 15, 10529–10566. <https://doi.org/10.5194/acp-15-10529-2015>.
- Talukdar, S., Singha, P., Mahato, S., Shahfahad Pal, S., Liou, Y.A., Rahman, A., 2020. Land-use land-cover classification by machine learning classifiers for satellite observations-A review. *Rem. Sens.* 12. <https://doi.org/10.3390/rs12071135>.
- Targino, A.C., Gibson, M.D., Krecl, P., Rodrigues, M.V.C., dosSantos, M.M., dePaula Corrêa, M., 2016. Hotspots of black carbon and PM_{2.5} in an urban area and relationships to traffic characteristics. *Environ. Pollut.* 218, 475–486. <https://doi.org/10.1016/j.envpol.2016.07.027>.
- Tsai, J.H., Huang, K.L., Lin, N.H., Chen, S.J., Lin, T.C., Chen, S.C., Lin, C.C., Hsu, S.C., Lin, W.Y., 2012. Influence of an Asian dust storm and Southeast Asian biomass burning on the characteristics of seashore atmospheric aerosols in Southern Taiwan. *Aerosol Air Qual. Res.* 12, 1105–1115. <https://doi.org/10.4209/aaqr.2012.07.0201>.
- U.S. EPA, 2014. Environmental Benefits Mapping and Analysis Program - Community Edition. Version 1.1.3 [WWW Document], 4.25.20. www.epa.gov/benmap.
- U.S. EPA, 2007. Guidance on the Use of Models and Other Air Quality Goals for Ozone, PM_{2.5}, and Regional Haze.
- U.S. EPA Office of Research and Development, 2017. CMAQ. <https://doi.org/10.5281/ZENODO.3585898>.
- Wang, C., Tu, Y., Yu, Z., Lu, R., 2015a. PM_{2.5} and cardiovascular diseases in the Elderly: an overview. *Int. J. Environ. Res. Publ. Health* 12, 8187–8197. <https://doi.org/10.3390/ijerph120708187>.
- Wang, J., Wang, S., Voorhees, A.S., Zhao, B., Jang, C., Jiang, J., Fu, J.S., Ding, D., Zhu, Y., Hao, J., 2015b. Assessment of short-term PM_{2.5}-related mortality due to different emission sources in the Yangtze River Delta, China. *Atmos. Environ.* 123, 440–448. <https://doi.org/10.1016/j.atmosenv.2015.05.060>.
- Weichenhath, S., Lavigne, E., Evans, G., Pollitt, K., Burnett, R.T., 2016. Ambient PM_{2.5} and risk of emergency room visits for myocardial infarction: impact of regional PM_{2.5} oxidative potential: a case-crossover study. *Environ. Heal. A Glob. Access Sci. Source* 15, 1–9. <https://doi.org/10.1186/s12940-016-0129-9>.
- Wernham, A., 2011. Health impact assessments are needed in decision making about environmental and land-use policy. *Health Aff.* 30, 947–956. <https://doi.org/10.1377/hlthaff.2011.0050>.
- World Health Organization, 2005. WHO Air Quality Guidelines for Particulate Matter, Ozone, Nitrogen Dioxide and Sulfur Dioxide: Global Update 2005 1–21. [https://doi.org/10.1016/0004-6981\(88\)90109-6](https://doi.org/10.1016/0004-6981(88)90109-6).
- Wu, P.-C., Cheng, T.-J., Kuo, C.-P., Fu, J.S., Lai, H.-C., Chiu, T.-Y., Lai, L.-W., 2020. Transient risk of ambient fine particulate matter on hourly cardiovascular events in Tainan City, Taiwan. *PLoS One* 15, e0238082. <https://doi.org/10.1371/journal.pone.0238082>.
- Xing, Y., Xu, Y., Shi, M., Lian, Y., 2016. The impact of PM_{2.5} on the human respiratory system. *J. Thorac. Dis.* 8, 69–74. <https://doi.org/10.3978/j.issn.2072-1439.2016.01.19>.

- Yorifuji, T., Suzuki, E., Kashima, S., 2014a. Hourly differences in air pollution and risk of respiratory disease in the elderly: a time-stratified case-crossover study. *Environ. Heal. A Glob. Access Sci. Source* 13, 1–11. <https://doi.org/10.1186/1476-069X-13-67>.
- Yorifuji, T., Suzuki, E., Kashima, S., 2014b. Cardiovascular emergency hospital visits and hourly changes in air pollution. *Stroke* 45, 1264–1268. <https://doi.org/10.1161/STROKEAHA.114.005227>.
- Zhang, Y., Foley, K.M., Schwede, D.B., Bash, J.O., Pinto, J.P., Dennis, R.L., 2019. A measurement-model fusion approach for improved wet deposition maps and trends. *J. Geophys. Res. Atmos.* 124, 4237–4251. <https://doi.org/10.1029/2018JD029051>.